

SHORT COMMUNICATION

WILEY

The effect of parked wind turbines on wind flow and turbulence over a complex terrain

Hrvoje Kozmar¹  | Gianni Bartoli²  | Claudio Borri² 

¹Faculty of Mechanical Engineering and Naval Architecture, University of Zagreb, Ivana Lučića 5, Zagreb, 10000, Croatia

²Department of Civil and Environmental Engineering, University of Florence, Via di Santa Marta 3, Florence, 50139, Italy

Correspondence

Hrvoje Kozmar, Faculty of Mechanical Engineering and Naval Architecture, University of Zagreb, Ivana Lučića 5, Zagreb, 10000, Croatia.
Email: hkozmar@fsb.hr

Funding information

FP7-Marinet; Croatian Science Foundation, Grant/Award Number: IP-2016-06-2017 (WESLO)

Abstract

Wind-tunnel experiments were performed to study the wind characteristics on a parked wind turbine downwind of three types of hill and over a flat terrain. The focus of the study is on comparing wind characteristics on (a) a wind turbine standing alone and (b) this same type of wind turbine embedded in a wind farm. Particular emphasis is placed on the hill size and shape and the distance between the hill and the wind farm. The hill and wind-farm models were subjected to an atmospheric boundary layer simulation to create realistic atmospheric conditions. Flow and turbulence were analyzed based on the measured mean flow velocity, Reynolds shear stress, turbulence intensity, and the power spectral density of velocity fluctuations. The experimental results reveal similar trends concerning (a) the wind characteristics obtained on a parked wind turbine embedded in a wind farm downwind of hills of various sizes and shapes and (b) the wind characteristics on this same type of parked wind turbine standing alone in the same position downwind of the same hills. In particular, the discrepancies in the mean flow velocity and turbulence intensity between these test cases are mostly below 5%, thus indicating that a complex terrain clearly has a dominant effect on the wind characteristics, while the effects of parked wind turbines on the wind characteristics are negligible. This important finding indicates that the structural loading of parked wind turbines situated on a complex terrain may be well calculated using the same procedures both for wind turbines standing alone and wind turbines embedded in wind farms if they are both placed at the same distance downwind of the same hills.

KEYWORDS

complex terrain, parked wind turbines, wind characteristics, wind farm, wind-tunnel experiments

1 | INTRODUCTION

Substantial knowledge is available concerning the aerodynamics of wind turbines situated on a flat terrain (FT) and in the open sea. Nevertheless, further work is still required to elucidate all the relevant details of the aerodynamic properties of wind turbines on a complex terrain to extend their lifetime and enhance energy production. One of the major issues is the effect of the terrain heterogeneity on wind flow and the turbulence experienced by wind turbines, for example, Porté-Agel et al.¹

This is an open access article under the terms of the Creative Commons Attribution License, which permits use, distribution and reproduction in any medium, provided the original work is properly cited.

© 2021 The Authors. *Wind Energy* published by John Wiley & Sons Ltd.

Previous studies indicated a clear need for this type of work because the wind characteristics of relevance to wind turbines are substantially different downwind of a hill than is the case on a FT, for example, Rokenes and Krogstad.² These terrain-induced flow alterations may have significant implications on the wind energy yield of wind turbines, for example, Prosper et al.³ Moreover, flow separating from the hill ridge and recirculating in its wake is strongly turbulent and characterized by exhibited spectral peaks of the turbulence kinetic energy (TKE) fluctuations, which are substantially different from those in the “standard” atmospheric boundary layer (ABL) developing over a FT. The TKE peak frequency may thus adversely arise in the range of natural frequencies characteristic of wind-turbine structures, may cause a non-Gaussian load, and may result in the damage or even collapse of these structures, for example, Botta et al.⁴ and Riziotis and Voutsinas.⁵

The scope of the present study is accordingly to investigate the wind characteristics concerning a parked wind turbine embedded in a wind farm downwind of a hill of three different sizes and shapes. Particular importance is given to studying realistic hill topographies similar to prototype conditions, because, in the past, wind characteristics have been mostly studied in relation to a generic bell-shaped hill, for example, Pirooz and Flay.⁶ The wind-turbine models were parked (not rotating) in all experiments in order to analyze the flow and turbulence characteristics in strong winds when the wind-turbine rotor blades stay still. All tests were also performed on a FT type (without the hill model) as a reference case. An attempt was also made to distinguish between the effects of parked wind turbines and hill orography on the wind characteristics over a complex terrain. This analysis complements previous findings concerning the wind characteristics related to wind turbines standing alone,^{7,8} those embedded in wind farms,⁹ and other aerodynamic aspects of parked wind turbines, Xu and Ishihara,¹⁰ Shirzadeh et al.,¹¹ and Tang et al.¹²

2 | EXPERIMENTAL SETUP

Experiments were carried out in a CRIACIV boundary layer wind tunnel, where the flow velocity can be regulated between 0 and 30 m/s using a 160-kW fan; the test section is 1.6 m high, 2.2 m wide, and 22 m long. More details on this wind tunnel are available in Augusti et al.¹³ The flow

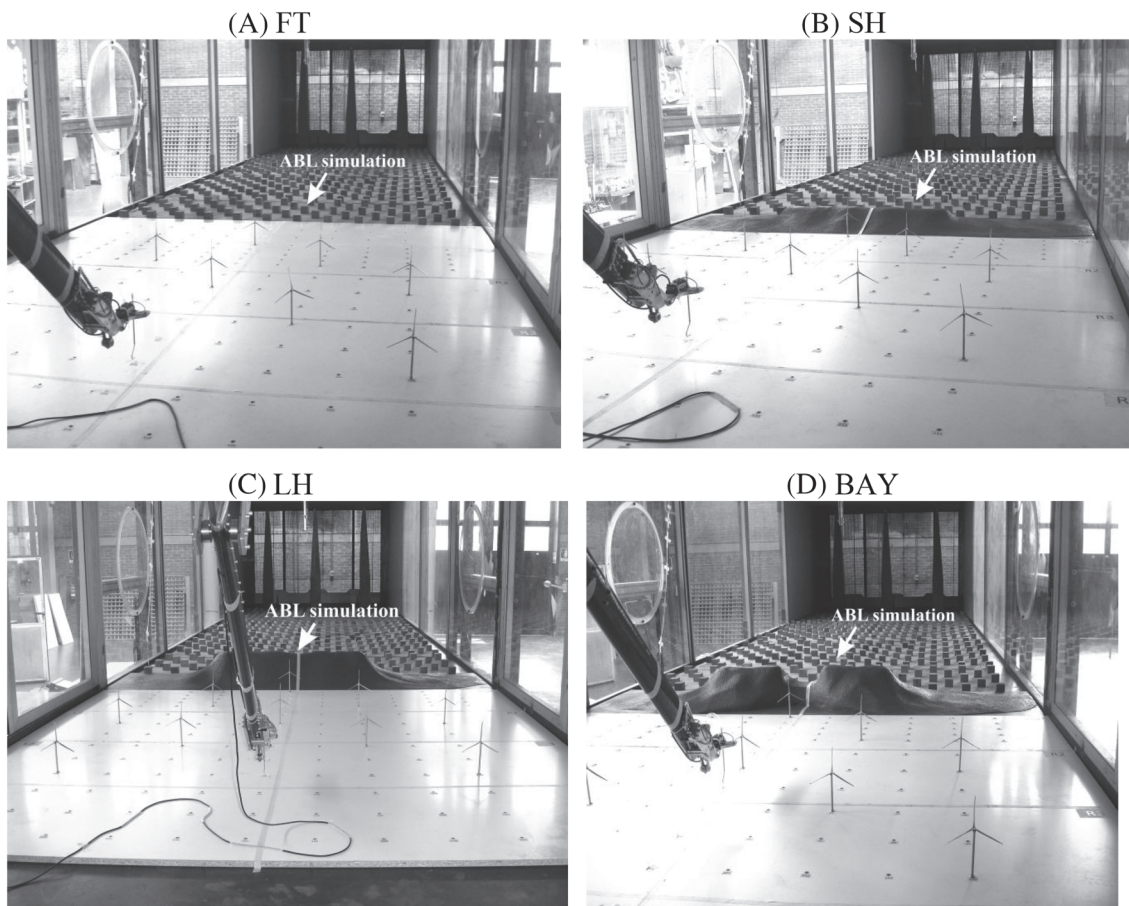


FIGURE 1 Arrangement of the ABL simulation, hill, and wind-farm models: (A) FT, (B) SH, (C) LH, and (D) BAY configurations

and turbulence characteristics over the hill models and around the wind-turbine models were determined using an Aeroprobe Cobra sensor, a conventional type of sensor with five holes and a maximum sampling rate of 50 Hz. A Prandtl-Pitot tube was used for reference velocity measurements in the freestream flow.

Experiments concerning the ABL simulation were performed at the time record length of 120 s, while the experiments with the hill and wind-farm models were carried out at the time record length of 60 s. The sampling rate was 500 Hz in all tests. The flow and turbulence characteristics were studied based on the mean flow velocity, turbulence intensity, Reynolds shear stress, and power spectral density of velocity fluctuations. The mean freestream velocity was $\bar{u}_\infty = 15.5$ m/s at 0.93-m height and 1 m upstream of the leading edge of the hill model.

The ABL simulation created using the Counihan¹⁴ method impinged on the hill and the wind-farm models, Figure 1. Three hill models were used to represent realistic terrains that commonly appear in the full scale, that is, small hill (SH), large hill (LH), and hill with a bay (BAY). The FT model was used as a reference case. Each hill model is 0.6 m long in the main flow direction and 1 m wide laterally to the main flow direction. The SH model is 0.1 m uniformly high, the LH model is 0.2 m uniformly high, while the BAY model is 0.2 m high, with its height decreasing to 0.1 m in

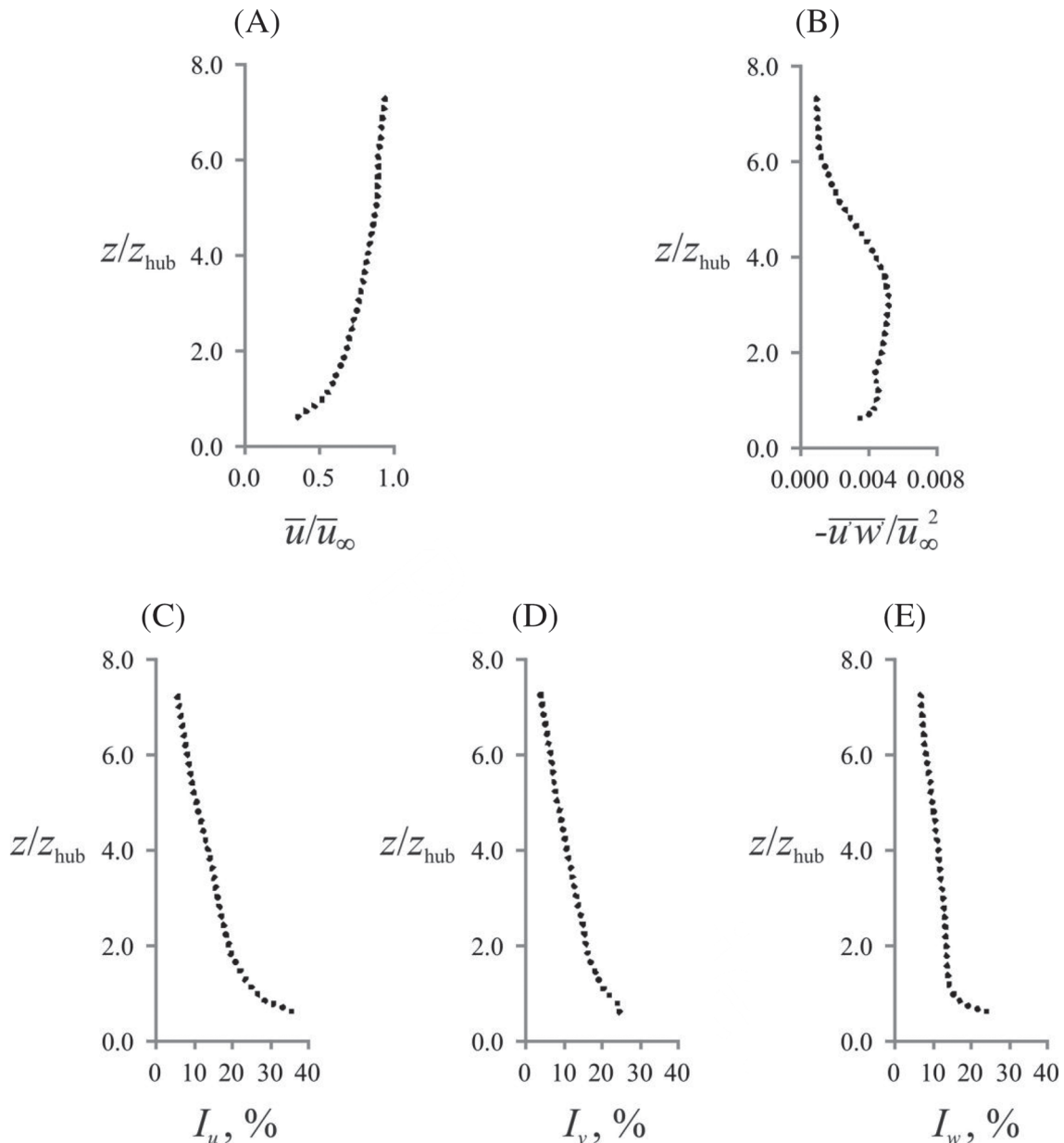


FIGURE 2 Characteristic profiles of the ABL simulation: (A) mean flow velocity, (B) Reynolds shear stress, and (C–E) longitudinal (I_u), lateral (I_v), and vertical (I_w) turbulence intensity normalized using the local mean flow velocity in the main flow direction at the measurement point height

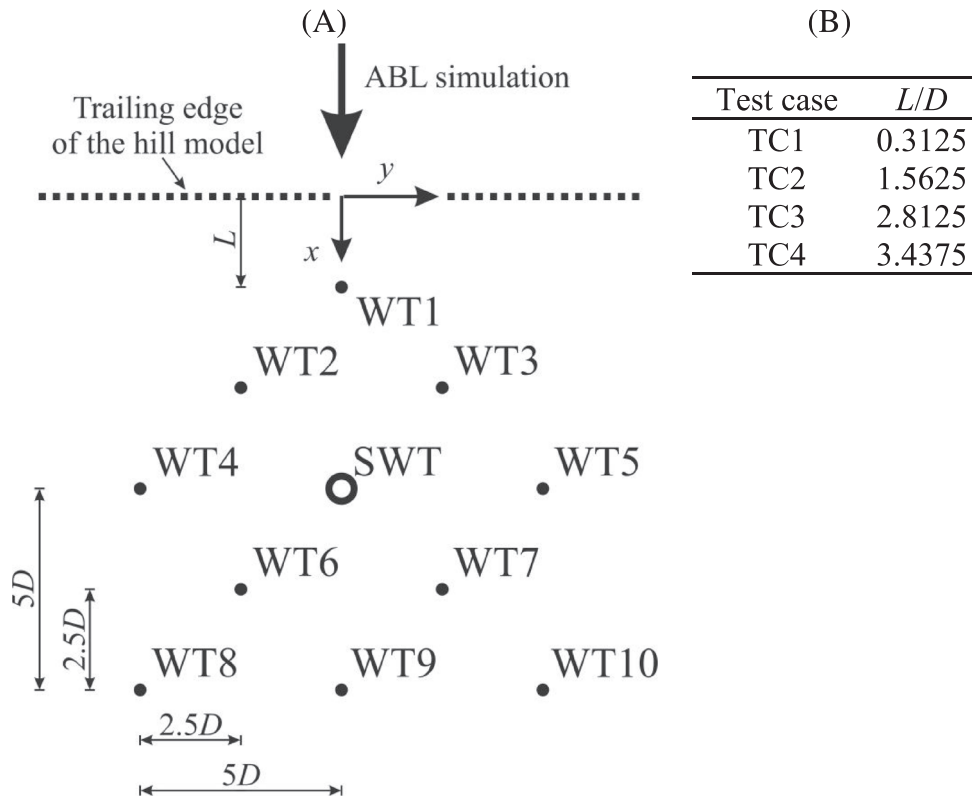


FIGURE 3 Experimental configurations: (A) layout of the ABL simulation, hill, and wind-farm models and (B) studied distances between the wind-farm and hill models

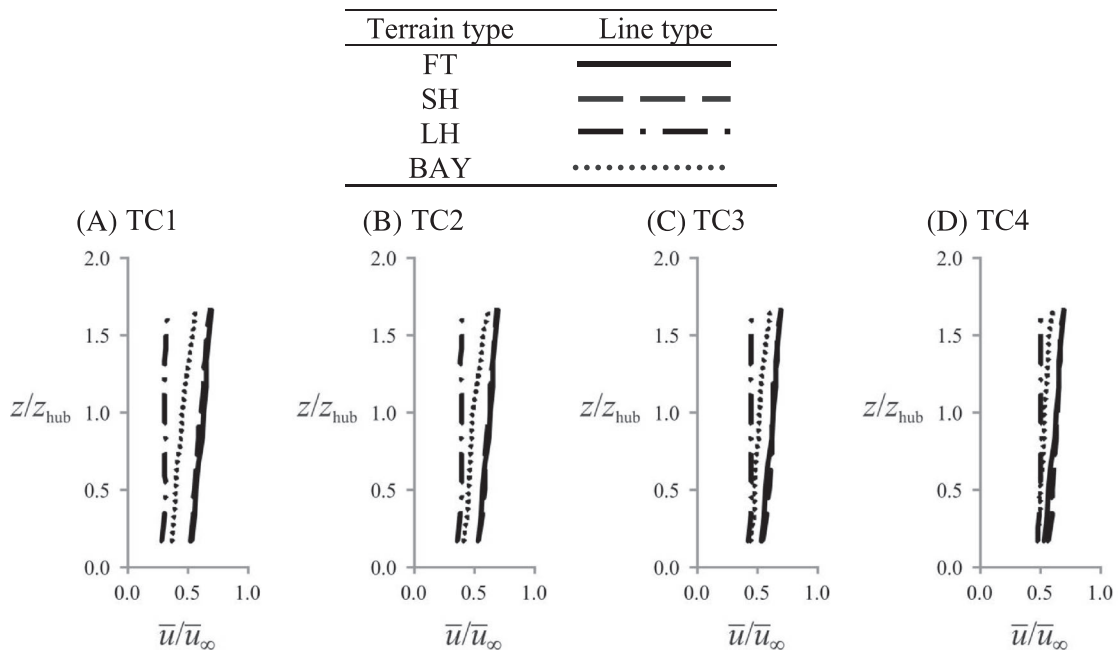


FIGURE 4 Mean flow velocity (\bar{u}) profiles in the TC1–TC4 configurations

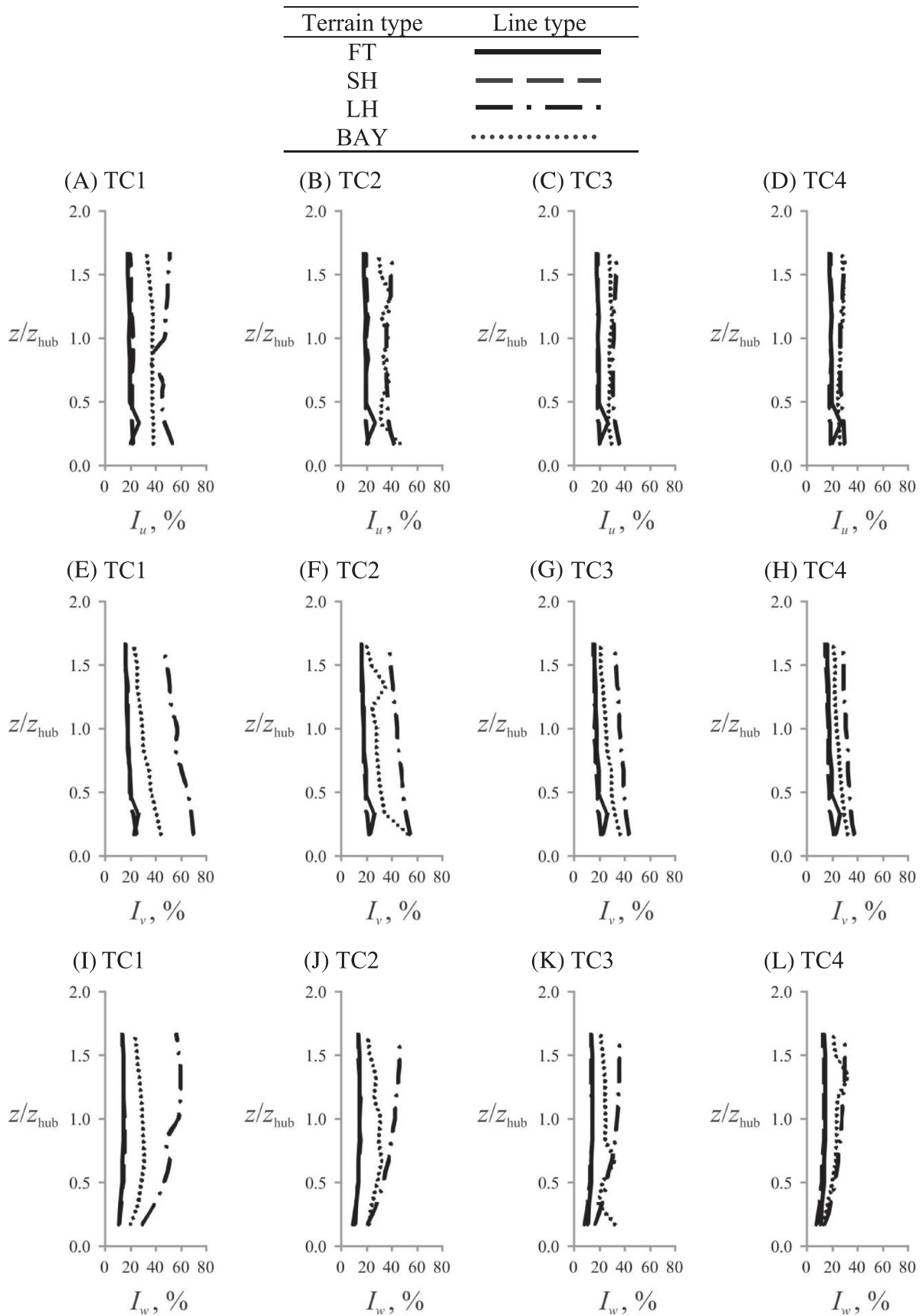


FIGURE 5 I_u , I_v , and I_w turbulence intensity profiles in the TC1–TC4 configurations

the lateral center of the hill model. The blockage of the test section was below 5% in all experiments, in agreement with Simiu and Scanlan¹⁵ and Holmes.¹⁶

The ABL simulation, which developed over the FT type and impinged on the hill and wind-farm models, is characterized by the mean flow velocity, Reynolds shear stress, and turbulence intensity profiles, Figure 2.

The ABL simulation length scale factor calculated as suggested by Cook¹⁷ is 300. The ABL parameters reported at the model scale are $z_0 = 6$ mm, $d = 50$ mm, and $\alpha = 0.26$, whose values were calculated using the procedure outlined in Kozmar.¹⁸

The wind-farm model consisted of 11 wind-turbine models arranged in a uniform, staggered pattern. However, there were only 10 wind-turbine models concurrently present in the test section because one wind-turbine model was removed from each experiment to determine the flow and turbulence characteristics on that particular wind-turbine model position. The wind-turbine models correspond to the Siemens 6.0-MW Sapiens wind turbine. The height of the cylindrical wind-turbine tower model is $z_{\text{hub}} = 120$ mm, and the tower model diameter is 6 mm. The 14-mm-long cylindrical nacelle model is 8 mm in diameter. Three $D/2 = R = 80$ -mm-long wind-turbine model blades were designed similar to DOWEC-NREL 5 MW and EU 56.1400-2 rotor blades ($D/z_{\text{hub}} = 4/3$). In order to satisfy the Jensen¹⁹ similarity, the ABL simulation length scale factor 300 calculated as suggested by Cook¹⁷ was adopted on the hill and wind-turbine models, as well.

In all experiments, the wind-turbine models were not rotating (parking position) in order to simulate the strong-wind situation at prototype wind speeds greater than 25 m/s. There were 10 measuring points distributed from the ground surface up to the top-tip height. The vertical distance between two neighboring measuring points was $z_{\text{hub}}/6$; that is, the measuring points were at 20, 40, 60, 80, 100, 120, 140, 160, 180, and 200 mm. The power spectra of the longitudinal velocity fluctuations were analyzed at three measuring points that correspond to the half-hub height (60 mm), hub height (120 mm), and top-tip height (200 mm) of the wind-turbine model. The ground plan of the ABL simulation, hill, and wind-farm models is shown in Figure 3; WT1–WT10 are dummy wind-turbine models, while SWT is the studied wind-turbine model position in the wind-farm model. The measurements were taken at the SWT position, which is located directly downstream of the lateral center of the hill model and the wind-tunnel test section.

Additional experiments were performed to distinguish between the effects of parked wind turbines and the hills on wind flow and turbulence over a complex terrain. In these experiments, the xy coordinates of the measuring points and the hill models were the same as those in Figure 3; the x , y , and z coordinate axes correspond to the u , v , and w velocity components, respectively. The measuring point was at a height corresponding to the wind-turbine model hub height.

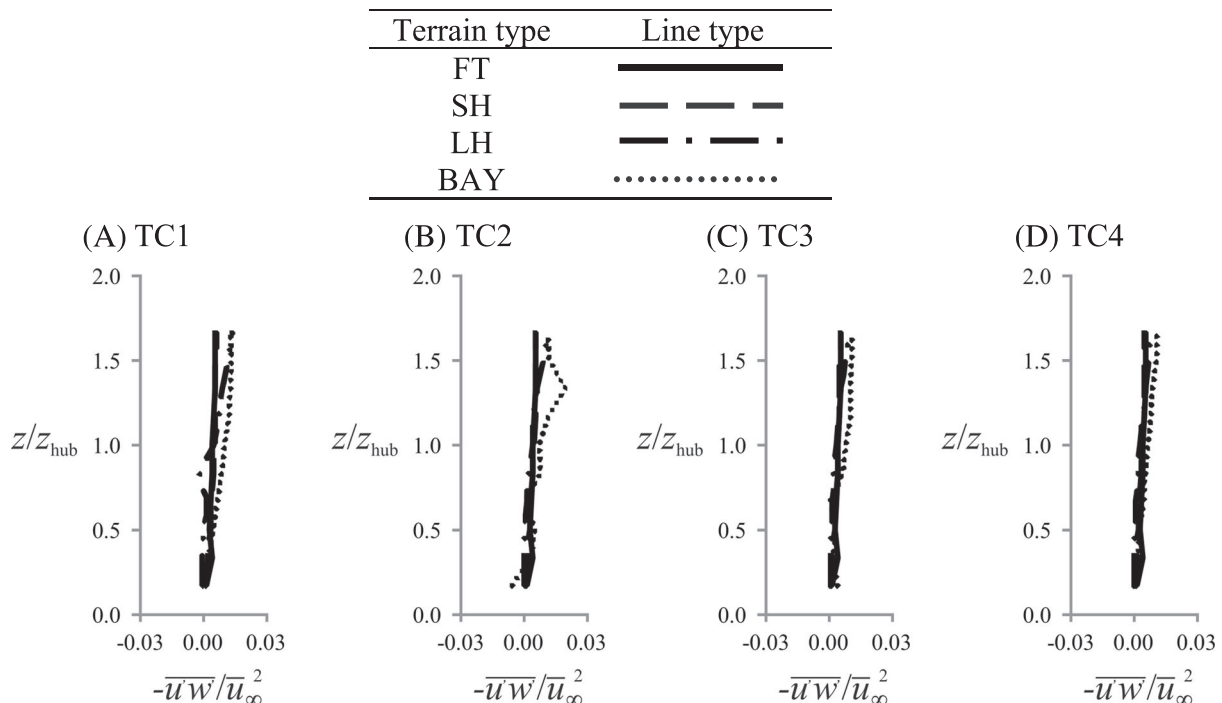


FIGURE 6 Reynolds shear stress ($-\overline{u'w'}$) profiles in the TC1–TC4 configurations

3 | RESULTS

Mean flow velocity and integral turbulence data are shown in Figures 4–6. The power spectra of the longitudinal velocity fluctuations are shown in Figures 7–9.

The results reported in Figures 4–9 indicate clear trends in the wind characteristics on a parked wind turbine embedded in a wind farm situated downwind of hills of various sizes and shapes. There is a substantial velocity reduction and turbulence enhancement in the hill wake exerted by the terrain orography, whose influences are more emphasized for larger hills of more complex orography, here LH and BAY. The terrain effect weakens further downwind of the hill; for example, the discrepancies in the experimental results at each respective height are substantially smaller in the TC4 than in the TC1 configuration.

The mean velocity profiles are generally rather uniform along the height, with an increasing mean velocity with the increasing height. The magnitude of the turbulence intensity is considerably larger than in the ABL. Immediately downwind of the hill, LH induces the largest turbulence intensity followed by BAY, while SH exhibits low turbulence intensity similar to FT. Unlike the ABL, where the turbulence intensity considerably decreases with the increasing height from the ground surface, downwind of the hill, the turbulence intensity remains fairly constant with the increasing height, or even increases in the case of I_w . The Reynolds stress remains nearly constant with the increasing height, with the exception of a strong gradient in BAY at TC2 above the hub height, likely due to a free shear layer separating from the hill ridge.

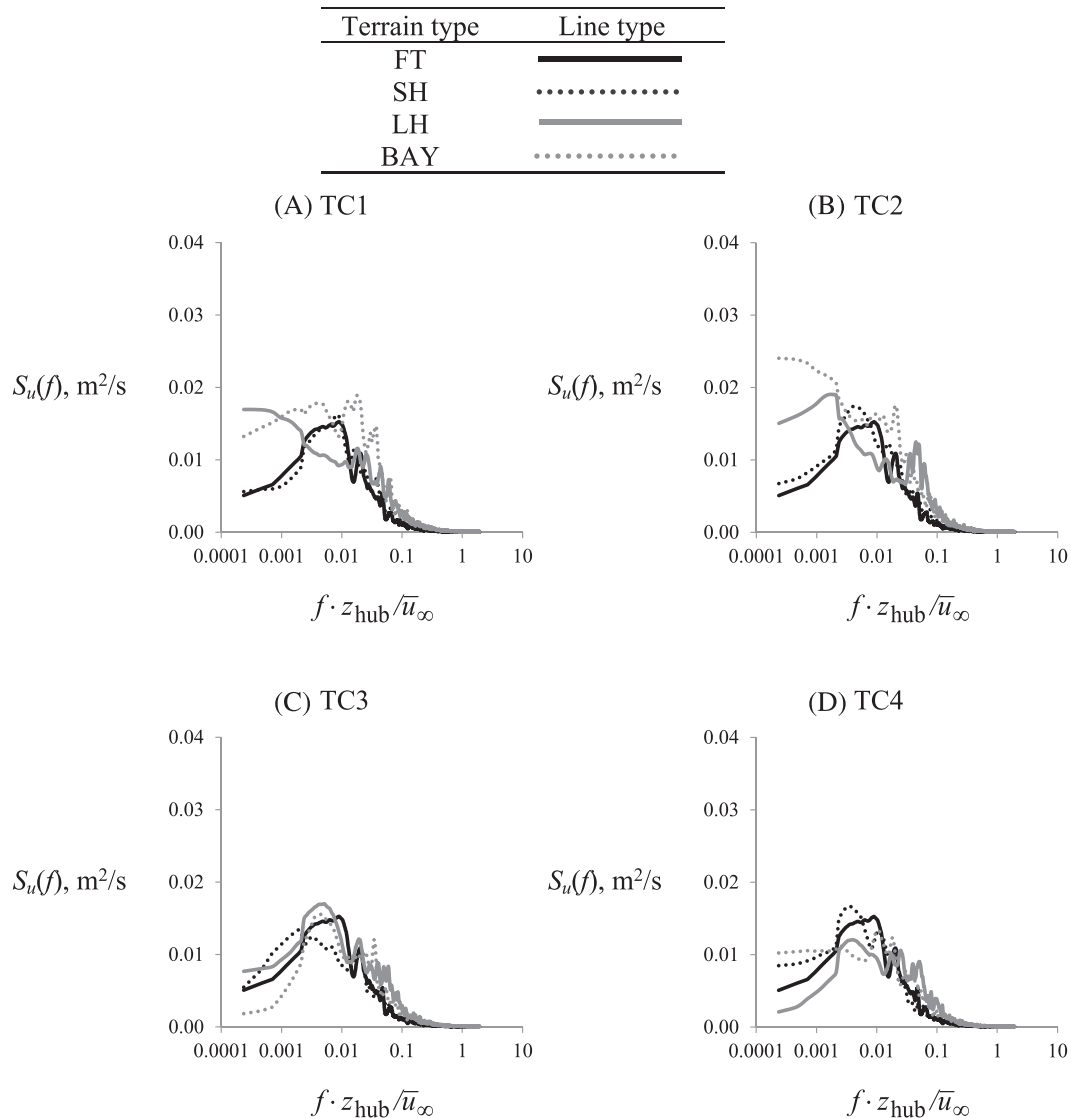


FIGURE 7 Power spectra of longitudinal velocity fluctuations at the half-hub height in the TC1–TC4 configurations

The peak values in the power spectra are predominantly exerted by the periodic vortex shedding from the hill, in agreement with previous field measurements, laboratory experiments and computational modeling, for example, Trischka,²⁰ Atkinson,²¹ and Schär and Smith.²² The spectral peak increases with the increasing height as the effect of the hill shadowing becomes smaller. Flow channeling through the hill pass (BAY) may yield a substantial additional unsteady loading that is not present with the uniform hill shapes, for example, Figures 8b and 9.

In order to distinguish between the effects of parked wind turbines and hills on the wind characteristics in a more quantitative manner, the absolute values of the discrepancies between the results obtained with and without the wind-farm model in the test section were normalized using the respective result obtained without the wind farm and presented for the mean flow velocity ($|\bar{u}_{WF} - \bar{u}_{NOWF}| / \bar{u}_{NOWF}$) and longitudinal turbulence intensity ($|I_{u,WF} - I_{u,NOWF}| / I_{u,NOWF}$), Table 1; \bar{u}_{WF} is the mean flow velocity at the wind-turbine model hub height with the wind-farm model surrounding the measuring position, \bar{u}_{NOWF} is the mean flow velocity at the wind-turbine model hub height without the wind-farm model surrounding the measuring position, and the same analogy is applied on the longitudinal turbulence intensity I_u . The discrepancies in the mean flow velocity \bar{u} and longitudinal turbulence intensity I_u shown in Table 1 are mostly below 5%, except for I_u in the BAY TC2 and BAY TC3 experiments due to the exhibited irregularities in the BAY orography, thus indicating that a complex terrain clearly has a dominant effect on the wind characteristics, while the effects of parked wind turbines on the wind characteristics are negligible.

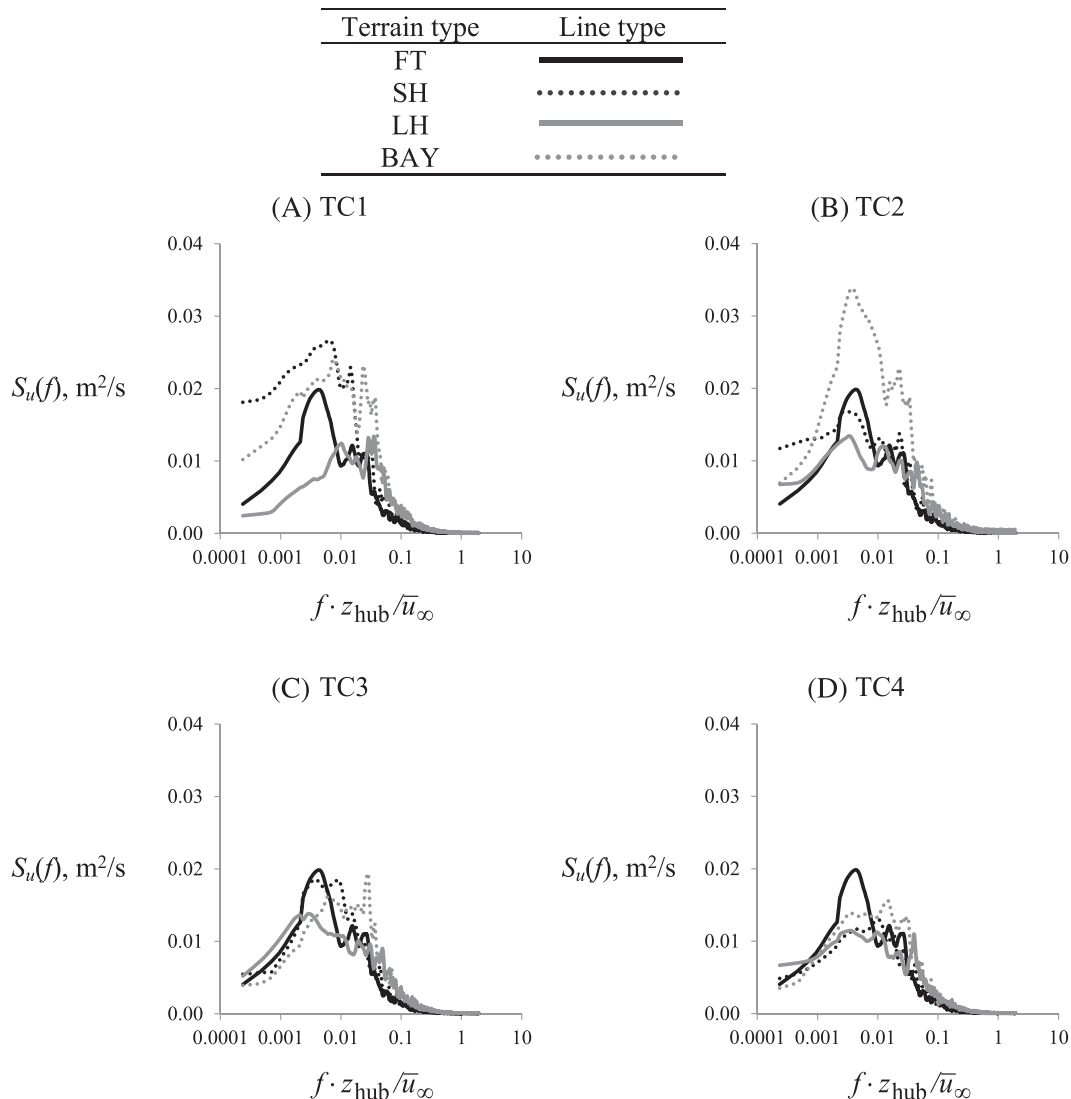


FIGURE 8 Power spectra of longitudinal velocity fluctuations at the hub height in the TC1–TC4 configurations

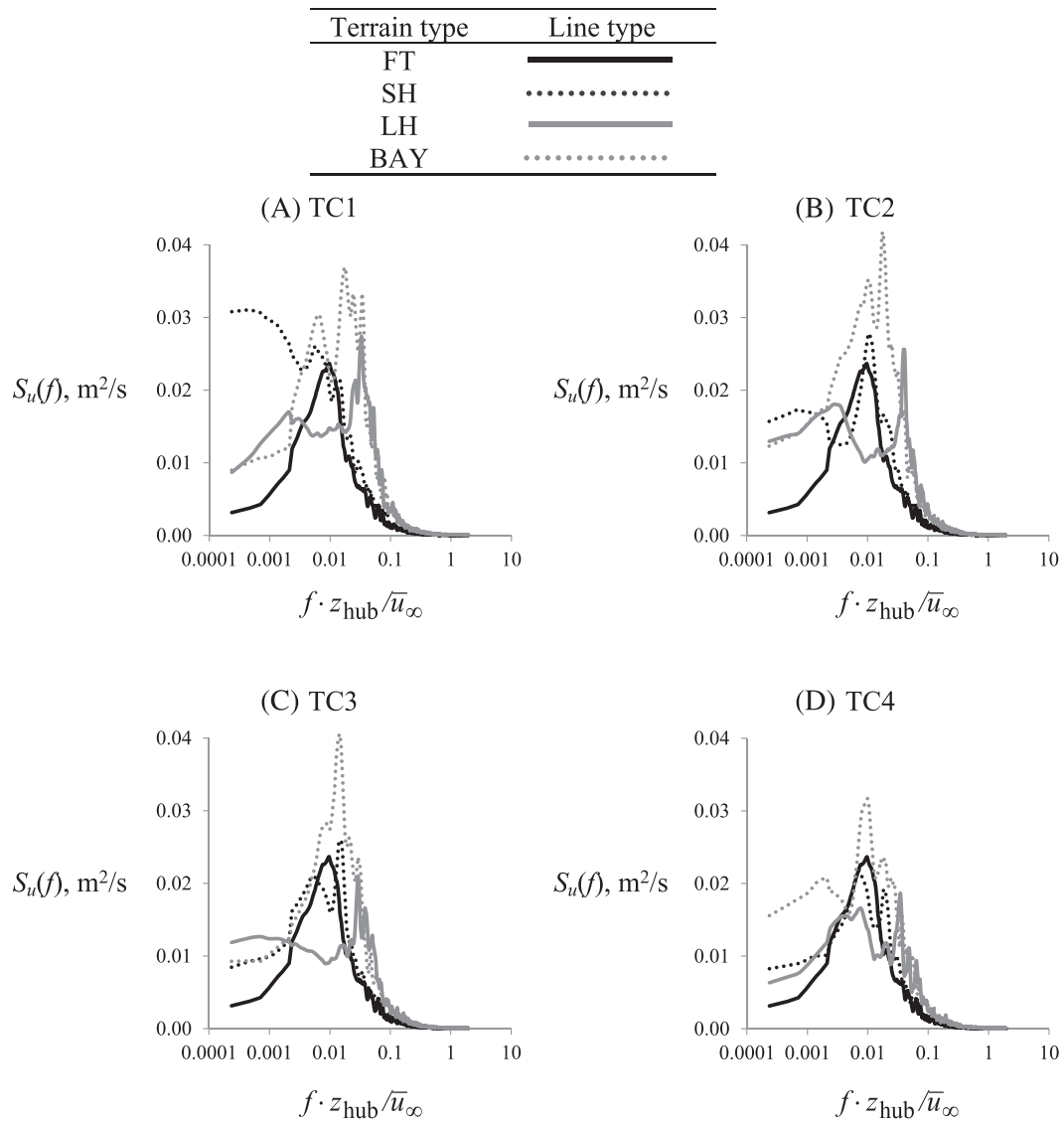


FIGURE 9 Power spectra of longitudinal velocity fluctuations at the top-tip height in the TC1–TC4 configurations

TABLE 1 Discrepancies in the mean flow velocity (\bar{u}) and longitudinal turbulence intensity I_u at the wind-turbine model hub height with and without the wind-farm model surrounding the measuring position

Test case	$ \bar{u}_{WF} - \bar{u}_{NOWF} / \bar{u}_{NOWF}$ (%)	$ I_{u,WF} - I_{u,NOWF} / I_{u,NOWF}$ (%)
FT TC1	0.0	3.6
SH TC1	1.1	0.0
SH TC2	1.0	3.4
SH TC3	1.0	1.6
SH TC4	2.0	4.5
LH TC1	4.3	5.3
LH TC2	1.7	4.5
LH TC3	1.4	0.6
BAY TC1	4.4	1.6
BAY TC2	2.7	16.0
BAY TC3	3.9	22.0
BAY TC4	1.2	4.3

4 | CONCLUSIONS

Wind-tunnel model experiments were performed to study wind characteristics on a parked wind turbine situated on a complex terrain. The experimental results reveal similar trends concerning (a) the wind characteristics obtained on a parked wind turbine embedded in a parked wind farm situated downwind of hills of various sizes and shapes and (b) the wind characteristics on this same type of parked wind turbine standing alone in the same position downwind of the same hills. The discrepancies in the mean flow velocity and turbulence intensity between the studied test cases are mostly below 5%, thus indicating that a complex terrain clearly has a dominant effect on the wind characteristics, while the effects of neighboring parked wind turbines on the wind characteristics are negligible. These discrepancies grow with an increase in the terrain complexity.

There is a substantial velocity reduction and turbulence enhancement in the hill wake exerted by the terrain orography, which is more emphasized for larger hills of more complex orography; this effect weakens further downwind of the hill. Flow channeling through the hill pass yields a substantial enhancement in the TKE magnitude, which may result in an additional unsteady loading of wind turbines at frequencies not observed with the uniform hill shapes.

These results indicate that the structural loading of parked wind turbines situated on a complex terrain may be well calculated using the same procedures both for wind turbines standing alone and wind turbines embedded in wind farms if they are both placed at the same distance downwind of the same hill. Future work will need to confirm these findings in a wider range of hill and wind-farm arrangements and inflow conditions.

ACKNOWLEDGEMENTS

The authors acknowledge FP7-Marinet and Croatian Science Foundation IP-2016-06-2017 (WESLO) funding. We thank Radoslav Babić, Milan Šulentić, Tomislav Barb, and Professor Nebojša Bojčetić and the Faculty of Mechanical Engineering and Naval Architecture, University of Zagreb, for their support concerning the manufacturing of the experimental models. Helpful discussions with Davide Allori, Claudio Mannini, and Enzo Marino are also greatly appreciated.

DATA AVAILABILITY STATEMENT

The data that support the findings of this study are available from the corresponding author upon reasonable request.

ORCID

Hrvoje Kozmar  <https://orcid.org/0000-0002-8490-3543>

Gianni Bartoli  <https://orcid.org/0000-0002-5536-3269>

Claudio Borri  <https://orcid.org/0000-0001-6660-2942>

REFERENCES

1. Porté-Agel F, Bastankhah M, Shamsoddin S. Wind-turbine and wind-farm flows: a review. *Bound-Lay Meteorol.* 2020;174(1):1-59.
2. Rokenes K, Krogstad P-Å. Wind tunnel simulation of terrain effects on wind farm siting. *Wind Energy.* 2009;12(4):391-410.
3. Prosper MA, Otero-Casal C, Fernandez FC, Miguez-Macho G. Wind power forecasting for a real onshore wind farm on complex terrain using WRF high resolution simulations. *Renew Energy.* 2019;135:674-686.
4. Botta G, Cavaliere M, Viani S, Pospíšil S. Effects of hostile terrains on wind turbine performances and loads: the Acqua Spruzza experience. *J Wind Eng Ind Aerod.* 1998;74-76:419-431.
5. Riziotis VA, Voutsinas SG. Fatigue loads on wind turbines of different control strategies operating in complex terrain. *J Wind Eng Ind Aerod.* 2000;85(3):211-240.
6. Pirooz AAS, Flay RGJ. Comparison of speed-up over hills derived from wind-tunnel experiments, wind-loading standards, and numerical modelling. *Bound-Lay Meteorol.* 2018;168(2):213-246.
7. Kozmar H, Allori D, Bartoli G, Borri C. Complex terrain effects on wake characteristics of a parked wind turbine. *Eng Struct.* 2016;110:363-374.
8. Kozmar H, Allori D, Bartoli G, Borri C. Wind characteristics in the wake of a non-rotating wind turbine close to a hill. *Trans Famena.* 2019;43(3):13-36.
9. Kozmar H, Allori D, Bartoli G, Borri C. Wind characteristics in wind farms situated on a hilly terrain. *J Wind Eng Ind Aerod.* 2018;174:404-410.
10. Xu N, Ishihara T. Analytical formulae for wind turbine tower loading in the parked condition by using quasi-steady analysis. *Wind Eng.* 2014;38(3):291-309.
11. Shirzadeh R, Weijtjens W, Guillaume P, Devriendt C. The dynamics of an offshore wind turbine in parked conditions: a comparison between simulations and measurements. *Wind Energy.* 2015;18(10):1685-1702.
12. Tang D, Xu M, Mao JF, Zhu H. Unsteady performances of a parked large-scale wind turbine in the typhoon activity zones. *Renew Energy.* 2020;149:617-630.
13. Augusti G, Spinelli P, Borri C, Bartoli G, Giachi M, Giordano S. The C.R.I.A.C.I.V. atmospheric boundary layer wind tunnel. In: Proceedings of the 9th International Conference on Wind Engineering (ICWE), New Delhi, India; 1995.
14. Counihan J. An improved method of simulating an atmospheric boundary layer in a wind tunnel. *Atmos Environ.* 1969;3(2):197-214.
15. Simiu E, Scanlan RH. *Wind Effects on Structures.* New York, USA: John Wiley & Sons; 1996.
16. Holmes JD. *Wind Loading of Structures.* 3rd ed. Taylor & Francis Group, Boca Raton, FL, USA: CRC Press; 2015.

17. Cook NJ. Determination of the model scale factor in wind-tunnel simulations of the adiabatic atmospheric boundary layer. *J Wind Eng Ind Aerod.* 1978;2(4):311-321.
18. Kozmar H. Physical modeling of complex airflows developing above rural terrains. *Environ Fluid Mech.* 2012;12(3):209-225.
19. Jensen M. The model law phenomena in natural wind. *Ingenioren.* 1958;2(4):121-128.
20. Trischka JW. Cone models of mountain peaks associated with atmospheric vortex streets. *Tellus.* 1980;32(4):365-375.
21. Atkinson BW. *Meso-scale Atmospheric Circulations.* London, UK: Academic Press; 1981.
22. Schär C, Smith RB. Shallow-water flow past isolated topography. Part 2: transition to vortex shedding. *J Atmos Sci.* 1993;50(10):1401-1412.

How to cite this article: Kozmar H, Bartoli G, Borri C. The effect of parked wind turbines on wind flow and turbulence over a complex terrain. *Wind Energy.* 2021;1-11. <https://doi.org/10.1002/we.2629>